



HAL
open science

Photorefractive response of CdTe:V under AC electric field from 1 to $1.5\mu\text{m}$

Yves Belaud, Philippe Delaye, Jean-Claude Launay, Gérald Roosen

► **To cite this version:**

Yves Belaud, Philippe Delaye, Jean-Claude Launay, Gérald Roosen. Photorefractive response of CdTe:V under AC electric field from 1 to $1.5\mu\text{m}$. *Optics Communications*, 1994, 105, pp.204-208. 10.1016/0030-4018(94)90716-1 . hal-00677548v1

HAL Id: hal-00677548

<https://hal-iogs.archives-ouvertes.fr/hal-00677548v1>

Submitted on 8 Mar 2012 (v1), last revised 30 Mar 2012 (v2)

HAL is a multi-disciplinary open access archive for the deposit and dissemination of scientific research documents, whether they are published or not. The documents may come from teaching and research institutions in France or abroad, or from public or private research centers.

L'archive ouverte pluridisciplinaire **HAL**, est destinée au dépôt et à la diffusion de documents scientifiques de niveau recherche, publiés ou non, émanant des établissements d'enseignement et de recherche français ou étrangers, des laboratoires publics ou privés.

PHOTOREFRACTIVE RESPONSE OF CdTe:V UNDER AC ELECTRIC FIELD FROM 1 TO 1.5 μ m

Yves Belaud¹, Philippe Delaye¹, Jean-Claude Launay², Gérald Roosen¹

1) Institut d'Optique Théorique et Appliquée, Unité de Recherche Associée 14 au Centre National de la Recherche Scientifique, Bât.503, Centre Scientifique d'Orsay, B.P.147, 91403 Orsay Cedex, France.

2) Pôle de Recherche Aquitain pour les Matériaux dans l'Espace (PRAME), B.P.11, 33165 Saint Médard en Jalles Cedex, France.

Classification :

42-65, 72-80E, 78-20J.

Abstract :

The AC field technique leading to the enhancement of the photorefractive effect is applied to Vanadium-doped Cadmium Telluride. Net photorefractive gain is obtained for the three wavelengths studied : 1.06 μ m, 1.32 μ m and 1.55 μ m. We observed a change in the sign of the photorefractive gain between 1.06 μ m and 1.55 μ m, which represents the first evidence of an electron-hole competition in this material. Theoretical interpretation is performed using an extension of the AC field theoretical model with bipolar conduction.

Introduction :

The development of optical communication networks and metrology systems at the eye-safe wavelength of $1.5\mu\text{m}$, increases the interest for the extension of the photorefractive effect towards the wavelength region of $1.3\text{-}1.5\mu\text{m}$. Cadmium Telluride (CdTe) appears to be a good candidate for such applications, as its sensitivity extends beyond $1.5\mu\text{m}$ and a photorefractive effect can be obtained with the low excitation energies delivered by lasers diodes [1-3]. In order to obtain the strong photorefractive gain necessary to exceed the threshold of the double phase conjugate mirror [4] (or other self pumped phase conjugate mirrors), the use of an externally applied electric field will be required. We perform a characterization of our sample performances using the two wave mixing technique and applying a square AC electric field. This AC field technique permits to keep the $\pi/2$ phase-shift which maximizes the two beam coupling photorefractive gain [5,6].

We here present the results of the study conducted at the three wavelengths $1.06\mu\text{m}$, $1.32\mu\text{m}$ and $1.55\mu\text{m}$. Net photorefractive gain is obtained at any of these wavelengths with applied field of $10\text{kV}\cdot\text{cm}^{-1}$ and field frequency around 100Hz . We obtain, for the first time to our knowledge in this kind of material, a change of the photorefractive majority carrier between the different wavelengths. We compare our experimental results to the theory, with a model of photorefractive effect with square AC field taking into account bipolar conduction (hole-electron competition).

Sample and experimental set-up presentations :

The CdTe sample we study was grown using modified Bridgman technique and Vanadium-doped with $1.5 \times 10^{19} \text{ at}\cdot\text{cm}^{-3}$. The dark conductivity is $6 \times 10^{-11} \Omega^{-1}\text{cm}^{-1}$. The absorption spectrum (Fig.1) clearly shows two absorption bands centered at $1\mu\text{m}$ and $1.5\mu\text{m}$, the last one extending up to $1.7\mu\text{m}$

The photorefractive effect is analysed in a two beam coupling geometry. The sources are diode-pumped Nd:YAG lasers emitting at $1.06\mu\text{m}$ and $1.32\mu\text{m}$ and a laser diode emitting at $1.55\mu\text{m}$. Two s-polarized beams, a strong pump I_p and a small probe I_s , interfere in the crystal ; the grating vector is oriented along (001) axis. The resulting space-charge field creates energy transfer from the pump to the probe. With a Ge photodiode, we measure the transmission of the probe beam with and without the presence of the pump and deduce the photorefractive gain Γ [7]. The interaction length of the crystal is $l = 0.866\text{cm}$. For this crystal, we previously reported on the variation of the photorefractive two beam coupling gain versus grating spacing without applied electric field [8]. This permitted to determine an effective trap density $N_{\text{eff}} = (1.2 \pm 0.3) \times 10^{15} \text{ cm}^{-3}$ and an electron-hole competition coefficient $\xi_0 = 0.51 \pm 0.06$ at $1.06\mu\text{m}$.

Using the method described in ref.[9], we determined that electrons were the majority carriers at this wavelength. The photorefractive gain at $1.32\mu\text{m}$ was found close to zero indicating a nearly perfect hole-electron compensation at this wavelength. Conducting now the same measurements at $1.55\mu\text{m}$, we obtain a gain $\Gamma = -0.09\text{ cm}^{-1}$ for a grating period of $\Lambda = 1.8\text{ }\mu\text{m}$. From this measurement we deduce an electron-hole competition coefficient $\xi_0 \approx -0.3$. This change in sign of the photorefractive gain gives an evidence of an electron-hole competition in this crystal with holes becoming a majority carriers at $1.55\mu\text{m}$ while electrons were majority carriers at $1.06\mu\text{m}$.

For AC field experiments, the electric field is applied along (001) through silver-painted electrodes. The field is given by a high voltage amplifier characterized by a slew-rate of $100\text{V}\cdot\mu\text{s}^{-1}$. The frequency of the square field is varied from 1Hz to 10kHz. The temporal shape of the field inside the crystal was checked by looking at the modulation of the transmission of the crystal placed between crossed polarizers (Pockels effect). At high frequency, the field is trapezoidal with a constant slope corresponding to the slew-rate value. At low frequency the field is perfectly square. We also checked that the field applied uniformly in the crystal with no high field regions across it.

Experimental results under AC field :

The photorefractive gain is influenced by different experimental parameters : the amplitude E_0 and the frequency F of the applied electric field, the pump to probe beam ratio β , the total incident illumination I_0 , the grating spacing Λ . We study the photorefractive gain variation versus these parameters.

Firstly the evolution of the photorefractive response with pump to probe beam ratio $\beta = I_p / I_s$ is conducted while maintaining a constant incident illumination. At $1.06\mu\text{m}$ and $1.55\mu\text{m}$ the gain continuously increases with this ratio (Fig.2) showing a saturation that occurs for β larger than 10^4 . This point will be discussed later. At $1.32\mu\text{m}$ due to the smaller value of the gain, the influence of β should be seen for smaller value of this ratio. Indeed we do not see any variation of the gain with β for the range of β of interest. For all the measurements we will present in the following, the pump to probe beam ratio is chosen high enough to be close to the saturation of the photorefractive gain.

We look at the variation of the gain with the applied electric field amplitude E_0 , for the different wavelengths (Fig.3). In all cases, the higher the field, the higher the photorefractive gain. The change of the sign of the photorefractive gain between $1.06\mu\text{m}$ and $1.55\mu\text{m}$, as well as the small gain at $1.32\mu\text{m}$ confirm the experiments performed without applied field in the same crystal. For all these measurements the frequency was optimized, i.e. the frequency was chosen high enough, compared to the

inverse of the photorefractive time constant, to reach the stationary regime [6].

Of course, this cutoff frequency will depend on both the applied electric field amplitude and the incident illumination. As predicted [6], we note that the cutoff frequency decreases with the amplitude of the applied electric field (fig.4). However for fields above 4 kV.cm⁻¹, we observe a non expected reduction of the plateau (Fig.4): the photorefractive gain decreases when we increase the frequency. This point will be discussed later. In the same way, as the response time of the photorefractive effect is inversely proportional to the incident illumination [7], the cutoff frequency will vary proportionally to this illumination [6]. We effectively observe such a variation (Fig.5) which gives a cutoff frequency of 30Hz for an incident illumination of 5mW.cm⁻² at 1.06μm for a field of 10 kV.cm⁻¹. At 1.55μm, the cutoff frequency is 5Hz for an incident illumination of 3mW.cm⁻² and a field of 10 kV.cm⁻¹ (see Fig.4).

At very low incident illumination the influence of the dark conductivity will decrease the gain. We can define the equivalent dark irradiance I_d as the irradiance at which the gain is reduced by a factor of 2. In our crystal, we measure $I_d \approx 50 \mu\text{W.cm}^{-2}$ at 1.32μm. At 1.06μm and 1.55μm, we could not reach a low enough illumination to observe a decrease of the gain. This value is equivalent to what was found in other crystals [1-3] and is coherent with the very low value of the dark conductivity we previously measured in this crystal [8].

Discussion :

In order to compare our experimental results with the theory, we use the model developed in [6] with the differential equations governing the space-charge field given by the electron-hole competition model [10]. When the frequency of the electric field overpass the cutoff frequency and the space-charge field is in the stationary regime, the expression of the photorefractive gain Γ reduces to :

$$\Gamma = \frac{2\pi n_0^3 r_{41} k_B T}{\lambda \cos \theta e} \left(\frac{k_0^2}{k} \right) \frac{(\alpha_n - \alpha_p) - (\alpha_n \kappa_n^2 I_n - \alpha_p \kappa_p^2 I_p)}{(\alpha_n + \alpha_p) + \alpha_n I_n (k_0^2 - \kappa_n^2) + \alpha_p I_p (k_0^2 - \kappa_p^2)}$$

$$\text{with : } I_n = \frac{k^2 + \kappa_n^2}{(k^2 + \kappa_n^2)^2 + k^2 V^2} \text{ and } I_p = \frac{k^2 + \kappa_p^2}{(k^2 + \kappa_p^2)^2 + k^2 V^2}.$$

$V = \frac{E_0 e}{k_B T}$, $\kappa_n^2 = \frac{e}{k_B T} \frac{1}{\mu_n \tau_n}$ and $\kappa_p^2 = \frac{e}{k_B T} \frac{1}{\mu_p \tau_p}$ $\mu_{n(p)}$ and $\tau_{n(p)}$ are the mobility and recombination time of electrons (holes). α_n and α_p are the parts of absorption that give electrons and holes respectively. They are deduced from the value of ξ_0 and α

according to the relations : $\alpha = \alpha_n + \alpha_p$ and $\xi_0 = \frac{\alpha_n - \alpha_p}{\alpha_n + \alpha_p}$. Taking a single

carrier model, the photorefractive gain expression reduces to the one found in ref.[5].

All the material parameters that influence the photorefractive gain through the theoretical expression are known except the recombination times τ_n and τ_p . The mobilities for electrons and holes are $\mu_n=520 \text{ cm}^2\text{V}^{-1}\text{s}^{-1}$ and $\mu_p=80 \text{ cm}^2\text{V}^{-1}\text{s}^{-1}$ [11]. The product $n_0^3 r_{41}$ is taken equal to 120 for the three wavelengths [1,2]. We thus adjust the theoretical curve to the experimental points for the three wavelengths by varying the values of τ_n and τ_p . At $1.06\mu\text{m}$ due to the electron dominated characteristic of the gain, the adjustment is more sensitive to τ_n , whereas at $1.55\mu\text{m}$ it is τ_p which is important as holes dominate. At $1.32\mu\text{m}$ where we have almost perfect electron-hole competition, theoretical gain is mainly sensitive to the ratio between τ_n and τ_p (fig.3). We determine from the adjustment : $\tau_n = 0.1\text{ns}$ and $\tau_p = 0.5\text{ns}$. The ξ_0 values used are : $\xi_0 = 0.51$ at $1.06\mu\text{m}$ as determined in previous experiments [8], $\xi_0 = 0.03$ at $1.32\mu\text{m}$ and $\xi_0 = -0.35$ at $1.55\mu\text{m}$ which correspond to the value we estimate from measurements at higher grating spacing. Using higher values for τ_n and τ_p will quickly give theoretical gains twice higher than experimental ones. For example, at $1.06\mu\text{m}$ the theoretical gain matches the experimental one (say 2.5 cm^{-1} at $5 \text{ kV}\cdot\text{cm}^{-1}$) with the above values of τ_n . Increasing τ_n by a factor of 2 leads to a photorefractive gain of 4.2 cm^{-1} , whereas a decrease by 2 gives a photorefractive gain of 1 cm^{-1} . This example indicates how sensitive to the values of τ_n and τ_p the adjustments are. The $\mu\tau$ products we deduce are: $\mu_n\tau_n=5\times 10^{-8}\text{cm}^2\text{V}^{-1}$ and $\mu_p\tau_p=4\times 10^{-8} \text{ cm}^2\text{V}^{-1}$; they are smaller than the one determined in other samples [1,2,12] but remain not too far from them.

For all these calculations we consider that the electric field is perfectly applied, i.e. $E_0=V_0/d$ with V_0 the applied voltage and d the interelectrode spacing. The effective applied field can possibly be smaller than V_0/d . Leaving E_0 as a variable parameter adds a degree of freedom for the adjustment of the experimental data. Taking a reduced value of the field leads to an increase of the possible values of τ_n and τ_p . However, as we do not know if this reduction of the internal field exists and what is its eventual strength, we decide to neglect this effect, as long as we don't have any evidence of its existence.

The experimentally observed decrease of the gain with increasing the field frequency is not predicted by the model developed in ref.[6] for a perfectly square field. A possible cause of this decrease can be the influence of the shape of the field, i.e. an influence of the slew-rate of the amplifier. To precise this influence we use the model developed in ref.[13] with the peculiar shape of our applied field. According to our calculation the photorefractive gain must decrease because of the slew-rate but this decrease should be noticeable only for frequencies higher than 500Hz. Our decrease occurs at about 100Hz at $1.06\mu\text{m}$ and around 30Hz at $1.55\mu\text{m}$ which are much lower

values than what we expect theoretically. The origin of this decrease of the gain is still unknown and is currently under study.

The variation of the photorefractive gain with the pump to probe beam ratio shows the evidence of the so called "large signal effect" [12,14]. Indeed our experimental results are not described by the classical law for the effective gain [7] : $\gamma_0 = \frac{1 + \beta}{1 + \beta e^{-\Gamma l}}$ (Fig.2). In the model for large signal effect, the transmission of the probe beam, in the case of undepleted pump, is given by [14] : $\frac{dI_s}{dz} = \Gamma \frac{f(m)}{m} I_s$ with the modulation $m \approx 2\beta^{-\frac{1}{2}}$ and with the function $f(m) = \frac{1}{a}(1 - \exp(-am))$. A good adjustment of our experimental results is obtained with this function (fig.2). The value we find for the coefficient a ($a=2.7$) is coherent with the data obtained in other kinds of materials like BGO [15], whose photorefractive parameters (N_{eff} , $\mu\tau$, ...) have similar values. All measurements shown on the other curves are conducted with a high pump to probe beam ratio in order to limit this large signal effect.

Conclusion :

We have presented here the first results of the photorefractive experiments we conducted on CdTe:V under applied AC field in the 1-1.5 μm range. The photorefractive gain we measure (5.5cm^{-1} at $1.06\mu\text{m}$ for a 10kV.cm^{-1}) already permits to overpass the threshold of double phase conjugate mirrors ($(\Gamma - \alpha)l > 4$) [4] with this sample. The results presented here are promising because of the low level of the illumination required (below 1mW.cm^{-2}) and the low frequency of the applied electric field (below 100Hz). We developed a model of photorefractive effect under applied AC field with two type of carriers that permits to explain most of our experimental results. We obtained the first evidence of an electron-hole competition in CdTe:V with a change of majority carrier between $1.06\mu\text{m}$ and $1.55\mu\text{m}$. Considering these first results a monopolar conductivity should be obtainable by varying growing or doping conditions. For example, doping of crystals with shallow acceptors would increase the role of holes, leading to optimum photorefractive properties at $1.55 \mu\text{m}$. Such an optimization work is currently under progress.

References :

- [1] A. Partovi, J. Millerd, E.M. Garmire, M. Ziari, W.H. Steier, S.B. Trivedi, M.B. Klein. Appl. Phys. Lett. **57**, (1990), 846.

- [2] J. C. Launay, V. Mazoyer, M. Tapiero, J.P. Zielinger, Z. Guellil, Ph. Delaye, G.Roosen. *Appl. Phys. A* **55**, (1992), 33.
- [3] M. Ziari, W.H. Steier, M.B. Klein, S.B. Trivedi. 3rd Topical Meeting on Photorefractive Materials, Beverly, 1991, Technical Digest **14**, p.159.
- [4] S. Weiss, S. Sternklar, B. Fisher. *Opt. Lett.* **12**, (1986), 114.
- [5] S.I. Stepanov, M.P.Petrov. *Opt. Comm.* **53**, (1985), 292.
- [6] C. Besson, J.M.C. Jonathan, A.Villing, G.Pauliat, G.Roosen. *Opt. Lett.* **14**, (1989), 1359.
- [7] N.V. Kukhtarev, V.B. Markov, S.G. Odulov, M.S. Soskin, V.L. Vinetskii. *Ferroelectrics* **22**, (1979), 949-961.
- [8] Ph. Delaye, F. Bignon, G.Roosen, M. Tapiero, J.P. Zielinger, Z. Guellil, J. C. Launay, V. Mazoyer. *Mol. Cryst. Liq. Cryst. Sci. Technol. - Sec.B. : Nonlinear Optics* **5**, (1993), in Press.
- [9] Ph. Delaye. "Etude des non-linéarités photoréfractives dans les composés semi-isolants III-V et II-VI : Influence d'une irradiation électronique" Thèse en Science Physique. Université Paris XI, Orsay (1993).
- [10] F.P. Strohkendl, J.M.C. Jonathan, R.W. Hellwarth. *Opt. Lett.* **11**, (1986), 312.
- [11] K. Jarasiunas, Ph. Delaye, J.C. Launay, G. Roosen. *Opt. Comm.* **93**, (1992), 59.
- [12] M. Ziari, W.H. Steier, P.M. Ranon, M.B. Klein, S.B. Trivedi. *J. Opt Soc. Am. B* **9**, (1992), 1461.
- [13] K. Walsh, A.K. Powell, C. Stace, T.J. Hall. *J. Opt Soc. Am. B* **7**, (1990), 288.
- [14] Ph. Refregier, L. Solymar, H. Rajbenbach, J.P. Huignard. *J. Appl. Phys.* **58**, (1985), 45.
- [15] N. Wolffer, P. Gravey, J.Y. Moisan, C. Laulan, J.C.Launay. *Opt. Comm.* **73**, (1989), 351.

Figure caption :

Figure 1 : Absorption spectrum of the CdTe:V sample

Figure 2 : Photorefractive amplification γ_0 (+, \times) as a function of the pump to probe beam ratio β at 1.06 μm and 1.55 μm . The thin line is the theoretical variation of γ_0 versus β according to the law $\gamma_0 = \frac{1 + \beta}{1 + \beta e^{-\Gamma}}$. The broad line correspond to the large signal effect curve(see text) with a coefficient $a=2.7$ at 1.06 μm and $a=2.2$ at 1.55 μm .

Figure 3 : Photorefractive gain Γ as a function of the applied AC field amplitude E_0 for the different wavelength 1.06 μm (+), 1.32 μm (\times) and 1.55 μm (o) The line represents the theoretical adjustment (see text). The frequency of the field is optimized for each value of E_0 , the experimental conditions are:

- at 1.06 μm : $\Lambda=10\mu\text{m}$, $\beta=10^4$, $I_{\text{inc}}=7\text{mW.cm}^{-2}$.
- at 1.32 μm : $\Lambda=21\mu\text{m}$, $\beta=270$, $I_{\text{inc}}=0.7\text{mW.cm}^{-2}$.
- at 1.55 μm : $\Lambda=11\mu\text{m}$, $\beta=780$, $I_{\text{inc}}=3.4\text{mW.cm}^{-2}$.

Figure 4 : Photorefractive gain as a function of the frequency F for different applied field at 1.06 μm and 1.55 μm : $E_0 = 2\text{kV.cm}^{-1}$ (+), $E_0 = 4\text{kV.cm}^{-1}$ (Δ), $E_0 = 6\text{kV.cm}^{-1}$ (\times), $E_0 = 10\text{kV.cm}^{-1}$ (\bullet).

Figure 5 : Variation of the optimal frequency as a function of the incident illumination I_{inc} at 1.06 μm ($\beta=10^4$, $E_0 = 10\text{kV.cm}^{-1}$, $\Lambda=10\mu\text{m}$).

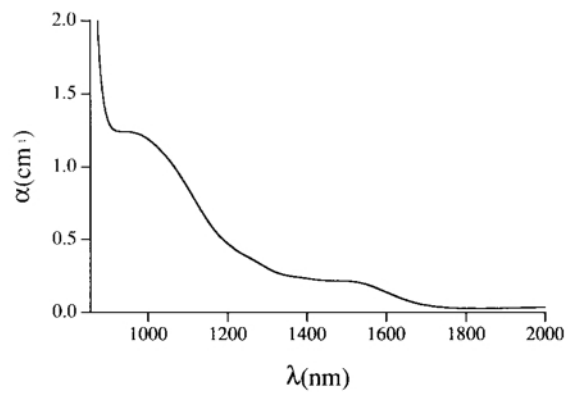


Figure 1

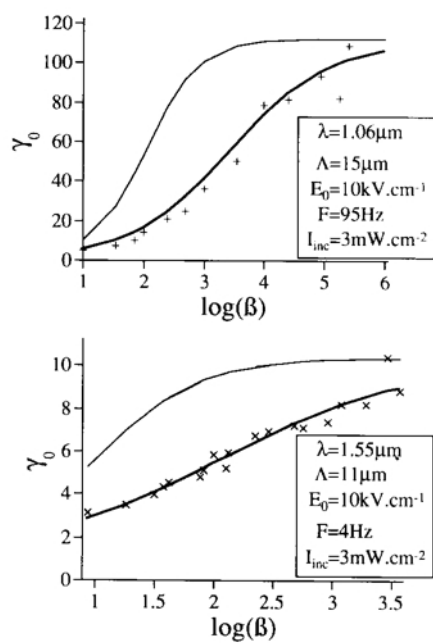


Figure 2

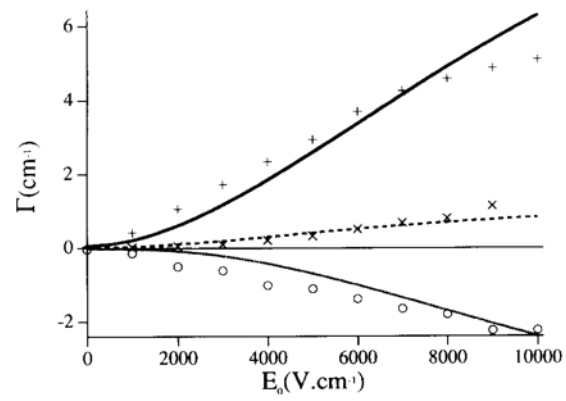


Figure 3

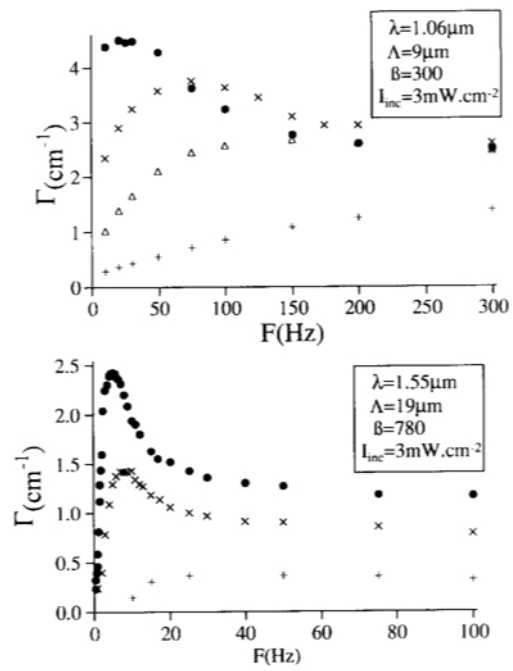


Figure 4

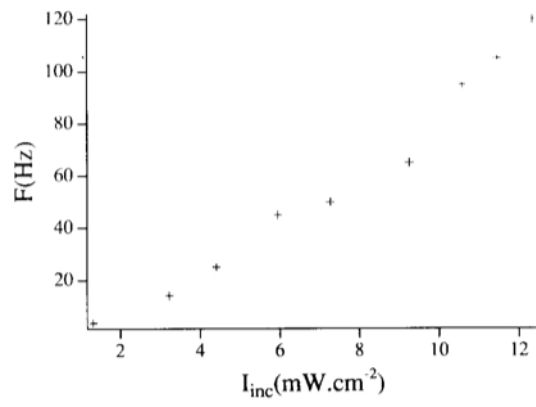


Figure 5